Conference paper

Dianna Himics*, Lukas Strizik, Jana Holubova, Ludvik Benes, Karel Palka, Bozena Frumarova, Jiri Oswald, Andrey S. Tverjanovich and Tomas Wagner

Physico-chemical and optical properties of Er^{3+}-doped and Er^{3+}/Yb^{3+}-co-doped $Ge_{25}Ga_{9.5}Sb_{0.5}S_{65}$ chalcogenide glass

DOI 10.1515/pac-2016-1103

Abstract: We investigated the physico-chemical properties, structure and optical properties of the $Ge_{25}Ga_{9.5}Sb_{0.5}S_{65}$: Er^{3+}/Yb^{3+} glasses. The Judd-Ofelt theory was used to calculate the intensities of the intra-4*f* electronic transitions of Er^{3+} ions. We observed the upconversion photoluminescence (UCPL) at 530, 550, 660 and 810 nm under 980 nm excitation. In the $Ge_{25}Ga_{9.5}Sb_{0.5}S_{65}$: 0.1 at.% Er^{3+}, we found that the Stokes photoluminescence (PL) at the green spectral region excited by the 490 and 532 nm laser is only ≈5 times higher than the UCPL emission under 810 or 980 nm excitation making these materials attractive for UCPL applications. The addition of 0.1–1 at.% of Yb^{3+} into $Ge_{25}Ga_{9.5}Sb_{0.5}S_{65}$: 0.1 at.% Er^{3+} glass reduces the UCPL as well as the Er^{3+} ≈1.5 μm emission intensity probably due to the reabsorption processes of the excitation light and concentration quenching. However, the observed Er^{3+}: ${}^4S_{3/2} \rightarrow {}^4I_{13/2}$ (≈850 nm) emission in the $Ge_{25}Ga_{9.5}Sb_{0.5}S_{65}$: 0.1 at.% Er^{3+} sample populates the ${}^4I_{13/2}$ level, which promises the using of this material for the 1.5 μm optical amplification.

Keywords: chalcogenide glasses; erbium; Ga-Ge-Sb-S; SSC-2016; upconversion photoluminescence; ytterbium.

Introduction

Rare-earth-doped chalcogenide glasses exhibit many interesting properties therefore, they are promising materials in variety of applications. Chalcogenide glasses (ChGs) possess low phonon energy and high refractive index [1–3] which suppresses the multiphonon relaxation and promotes radiative recombination, respectively [4]. Moreover, ChGs are transparent from visible to mid-infrared spectral region and show large intra-4*f* cross sections when they are doped with rare-earth (RE) ions [5]. RE^{3+}-doped ChGs can be applied such as optical amplifiers [6], waveguides [7], displays [8], sensors and detectors [9–11], lasers [12, 13].

The Er^{3+}: ${}^4I_{13/2} \rightarrow {}^4I_{15/2}$ (λ≈1.5 μm) near-infrared emission has attracted the attention in telecommunication *C*-band [14, 15]. To improve the efficiency of the ≈1.5 μm emission, the Er^{3+} ions can be co-doped with the Yb^{3+} ions, where Yb^{3+} ions play role of the sensitizer at pumping wavelength of ≈980 nm and allow the energy

Article note: A collection of invited papers based on presentations at the 12th Conference on Solid State Chemistry (SSC-2016), Prague, Czech Republic, 18–23 September 2016.

***Corresponding author: Dianna Himics,** Department of General and Inorganic Chemistry, Faculty of Chemical Technology, University of Pardubice, Studentska 573, 53210 Pardubice, Czech Republic, e-mail: dianna.himics@student.upce.cz
Lukas Strizik, Jana Holubova, Ludvik Benes, Karel Palka and Tomas Wagner: Department of General and Inorganic Chemistry, Faculty of Chemical Technology, University of Pardubice, Studentska 573, 53210 Pardubice, Czech Republic
Bozena Frumarova: Institute of Macromolecular Chemistry of Czech Academy of Sciences, v.v.i., Heyrovskeho nam. 2, 162 06 Prague, Czech Republic
Jiri Oswald: Institute of Physics of the ASCR, v.v.i., Cukrovarnicka 10, 16200 Prague, Czech Republic
Andrey S. Tverjanovich: Department of Laser Chemistry and Laser Material Science, Saint Petersburg State University, Universitetskii pr. 26, 198504 Saint Petersburg, Russia

transfer to neighboring Er^{3+} ions. It was demonstrated that the Er^{3+}/Yb^{3+} co-doping has become an effective method for production of short amplifiers and efficient lasers in the long haul telecommunications [16, 17]. The efficient $Yb^{3+}\rightarrow Er^{3+}$ energy transfer was first investigated by Snitzer and Woodcock in Na-K-Ba silicate glasses [17]. Recently, Er^{3+}/Yb^{3+} -co-doped fiber lasers [17, 18] and planar waveguide amplifiers [14, 16, 19] have been demonstrated.

In this paper, we have chosen the Ga-Ge-Sb-S chalcogenide glasses as the promising host matrix for the RE^{3+} ions [20, 21]. The addition of Sb into Ge-Ga-S glasses improves the resistance against crystallization and resistance to moisture with still large solubility of the RE^{3+} ions due to the presence of Ga [20, 22]. Reference [21] reports the effect of compositional changes in $Ge_{25}Ga_{10-x}Sb_xS_{65}$: 0.5 at.% Er^{3+} on the upconversion photoluminescence (UCPL). In the present study, we aim on the UCPL and ≈1.5 μm photoluminescence (PL) emission in $(Ge_{0.25}Ga_{0.095}Sb_{0.005}S_{0.65})_{99.9-x}Er_{0.1}Yb_x$, where $x = 0$, 0.1, 0.5 and 1.0 at.% and $(Ge_{0.25}Ga_{0.095}Sb_{0.005}S_{0.65})_{99.85}Er_{0.05}Yb_{0.1}$ (further denoted as Ga-Ge-Sb-S: Er^{3+}/Yb^{3+}) chalcogenide glasses with respect to their optical properties and structure.

Experimental

The $(Ge_{0.25}Ga_{0.095}Sb_{0.005}S_{0.65})_{99.9-x}Er_{0.1}Yb_x$ ($x = 0$, 0.1, 0.5, 1) and $(Ge_{0.25}Ga_{0.095}Sb_{0.005}S_{0.65})_{99.85}Er_{0.05}Yb_{0.1}$ ChGs were synthesized from high-purity elements of Ge (5N), Ga (5N), Sb (5N), S (4.5N), Er (3N) and Yb (3N). Elements were weighted into silica ampoules, which were sealed at residual pressure of ~10^{-3} Pa. The total weight of batch was 10 g. The sealed ampoules were heated at 1270 K for 24 h in a rocking furnace. The melt of the glass was quenched into water and the glass was annealed at 20 K below the glass transition temperature T_g for 2 h to relax the mechanical strain. Finally, the prepared samples were cut into discs with diameter of ≈10 mm and thickness ≈2–4 mm and polished into optical quality.

The non-crystalline nature of prepared glasses has been confirmed by X-ray diffraction (XRD) analysis using the Bruker D8 advance powder XRD diffractometer. The XRD investigation with Cu $K\alpha$ radiation was carried out on the as-prepared and annealed glasses in the 2θ range of 5–65° with a step of 0.02°. The compositions of prepared glasses were characterized by the energy dispersive X-ray (EDX) microanalyzer Aztec X-Max 20, Oxford Instruments at accelerating voltage of 20 kV. Differential scanning calorimeter DSC Diamond, Perkin-Elmer was employed to investigate thermal properties of the studied glasses in the range of 570–870 K and at heating rate of 10 K min^{-1}. A piece of glass about ≈10 mg was sealed into an aluminum pan for the measurement. The glass transition temperature (T_g) was determined as half-height between extrapolated onset and endset, the crystallization temperature (T_c) as onset of crystallization peak.

The Raman spectra were measured under the Nd:YAG laser ($\lambda = 1064$ nm) excitation at room temperature using the FT-IR spectrophotometer IFS 55 with the Raman FRA-106 accessory (Bruker) for back scattering geometry. Raman spectra were reduced by the Gammon-Shuker approximation [23] and decomposed into individual bands by the pseudo-Voigt functions.

Archimedes method was used for determination of the density of prepared glasses. Refractive index of glasses was determined by the variable angle spectroscopic ellipsometry (VASE, J.A. Woollam Co., Inc.) measured in the spectral region of 500–2300 nm with a spectral step of 20 nm and at angles of light incidence 65°, 70°, 75°. The ellipsometric data were parameterized by the Sellmeier model [24] in transparent spectral region of studied materials with obtained fit accuracy given by the mean square errors <1.5. Er^{3+} and Yb^{3+} absorption cross sections spectra were determined using the double-beam UV-Vis-NIR spectrophotometer (JASCO V-570) in the spectral region of 300–2500 nm with a spectral step of 2 nm. Intensities of the Er^{3+} intra-4*f* electronic transitions in the $Ge_{25}Ga_{9.5}Sb_{0.5}S_{65}$ host matrix were calculated by the Judd-Ofelt theory [25–28] using the Er^{3+} absorption bands centered at 1538, 989, 815, 661, 545, and 522 nm and JOF program v. 2.3 [25, 26, 29]. The areas of absorption bands were fitted by Gausssians in Fityk program v. 0.9.8 [30]. The Er^{3+} 1.5 μm PL emission spectra of the Ga-Ge-Sb-S: Er^{3+}/Yb^{3+} ChGs were measured in the spectral region of 1440–1650 nm with a 0.5 nm step and excited by the 980 nm diode laser (power density ≈80 W cm^{-2}). PL signal was processed with a 1/2 m

double grating monochromator and amplified by preamplifier and lock-in amplifier at chopping frequency of 30 Hz. The PL signal was detected under 90° by the two-step-cooled Ge detector. PL and UCPL emission spectra measured in the spectral region of 500–900 nm with a 0.5 nm step were acquired at pumping wavelengths of 490, 532, 810 and 980 nm using the Ti:sapphire laser (power density ≈3800 W cm^{-2}) pumped with Nd:YVO_4. The PL signal was processed through 1/8 m monochromator and detected by the GaAs photomultiplier tube. All photoluminescence measurements were carried out at room temperature.

Results and discussion

All measured XRD patterns presented in Fig. 1 confirmed the amorphous state of the prepared Ga-Ge-Sb-S: Er^{3+}/Yb^{3+} ChGs.

The chemical composition of $(Ge_{0.25}Ga_{0.095}Sb_{0.005}S_{0.65})_{99.9-x}Er_{0.1}Yb_x$ ($x = 0$, 0.1, 0.5, 1) and $(Ge_{0.25}Ga_{0.095}Sb_{0.005}S_{0.65})_{99.85}Er_{0.05}Yb_{0.1}$ ChGs determined by the EDX spectroscopy is shown in Table 1. The observed results show a small deviation between experimental and theoretical chemical composition.

The temperature difference ΔT between the crystallization temperature $T_c \approx 837$ K and the glass transition temperature $T_g \approx 713$ K is >100 K suggesting the good thermal stability of synthesized glass. By the thermal stability is meant a broader temperature range at which the glass can be processed such as for fibers drawing.

Densities of prepared ChGs determined by the Archimedes method are shown in the Table 2. Densities were further used to calculate the concentration of Er^{3+} and Yb^{3+} ions per unit volume in $Ge_{25}Ga_{9.5}Sb_{0.5}S_{65}$ glass (see Table 2). The density of Ga-Ge-Sb-S ChGs increases with increasing Yb and Er content [31].

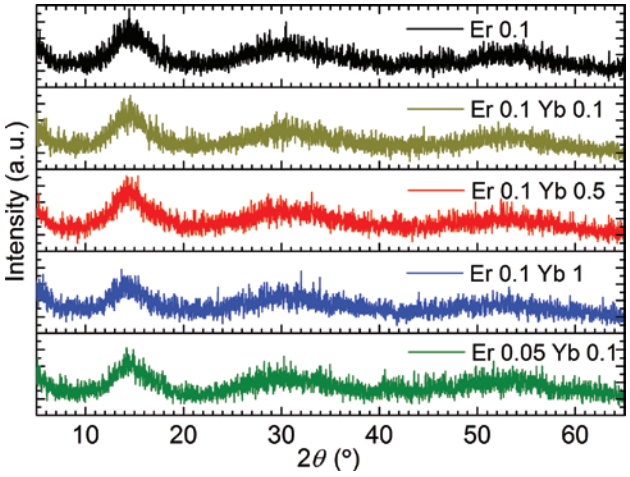

Fig. 1: XRD patterns for Ga-Ge-Sb-S: Er^{3+}/Yb^{3+} chalcogenide glasses. (color online).

Table 1: Chemical composition of $Ge_{25}Ga_{9.5}Sb_{0.5}S_{65}$ chalcogenide glasses doped with Er^{3+} or Er^{3+}/Yb^{3+} ions. The error of EDX spectroscopy measurements is ±1 at.%.

Sample	Chemical composition					
	Ge (at.%)	Ga (at.%)	Sb (at.%)	S (at.%)	Er (at.%)	Yb (at.%)
Er0.1	25.(0)	7.(9)	0.(5)	66.(5)	–	–
Er0.1Yb0.1	23.(7)	10.(2)	0.(5)	65.(6)	–	–
Er0.1Yb0.5	22.(3)	11.(4)	0.(6)	65.(0)	–	0.(7)
Er0.1Yb1	24.(1)	9.(3)	0.(5)	65.(3)	–	0.(9)
Er0.05Yb0.1	24.(2)	9.(2)	0.(5)	66.(1)	–	–

Table 2: Physical properties of $(Ge_{0.25}Ga_{0.095}Sb_{0.005}S_{0.65})_{99.9-x}Er_{0.1}Yb_x$ ($x=0$, 0.1, 0.5, 1) and $(Ge_{0.25}Ga_{0.095}Sb_{0.005}S_{0.65})_{99.85}Er_{0.05}Yb_{0.1}$ chalcogenide glasses.

Sample	$Er_{0.1}$	$Er_{0.1}Yb_{0.1}$	$Er_{0.1}Yb_{0.5}$	$Er_{0.1}Yb_1$	$Er_{0.05}Yb_{0.1}$
Density (g cm^{-3})	2.909 ± 0.004	2.943 ± 0.006	2.981 ± 0.007	3.014 ± 0.006	2.914 ± 0.007
Er^{3+} ions concentration ($\times10^{19}$ cm^{-3})	3.822 ± 0.006	3.837 ± 0.008	3.822 ± 0.009	3.836 ± 0.008	1.912 ± 0.004
Yb^{3+} ions concentration ($\times10^{19}$ cm^{-3})	–	3.842 ± 0.008	19.222 ± 0.004	38.391 ± 0.008	3.822 ± 0.008
Refractive index *n* (at 663 nm)	2.09 ± 0.01	2.09 ± 0.01	2.10 ± 0.01	2.13 ± 0.01	2.09 ± 0.01

Moreover, the refractive index determined by the VASE slightly increases with increasing concentration of Yb^{3+} ions (Table 2).

The structure of the $Ge_{25}Ga_{9.5}Sb_{0.5}S_{65}$ glass doped with 0.1 at.% Er was investigated by Raman spectroscopy, as shown in Fig. 2. The spectrum was decomposed into several bands. The main and the most intense Raman band near 340 cm^{-1} can be assigned to a ν_1 vibrational mode of the corner-sharing $GeS_{4/2}$ and $GaS_{4/2}$ tetrahedra. The small band at 265 cm^{-1} can be associated with vibrations of the metal–metal bonds in $S_3Ge(Ga)$-$Ge(Ga)S_3$ structural units. The band with maximum near of 375 cm^{-1} can be assigned to the ν_1 mode of two edge shared tetrahedra $Ge_2S_4S_{2/2}$ and $Ga_2S_4S_{2/2}$. The last two bands located at 400 and 435 cm^{-1} correspond to the ν_3 modes of the corner-sharing and edge- sharing $GeS_{4/2}$ and $GaS_{4/2}$ tetrahedra. Broad band in the region of 80–230 cm^{-1} does not show any fine structure and thus, it is difficult to decompose it into individual bands. However, the ν_2 and the ν_4 vibrational modes of the corner-sharing $GeS_{4/2}$ and $GaS_{4/2}$ originate at this spectral region. We did not find any band which can be associated with vibrational modes of Sb-based structural units, probably due to the low concentration of Sb (<1 at.%) in the studied glasses.

Absorption coefficients of the Er^{3+}-doped and the Er^{3+}/Yb^{3+}-co-doped $Ge_{25}Ga_{9.5}Sb_{0.5}S_{65}$ glasses are shown in Fig. 3. We observed the ground state absorption (GSA) bands of Er^{3+} centered approximately at 1538, 979, 815, 661, 545, and 522 nm. One strong GSA band at 992 nm originates from Yb^{3+}: $^2F_{7/2}\rightarrow{}^2F_{5/2}$ transitions and this band overlaps with the Er^{3+}: $^4I_{15/2}\rightarrow{}^4I_{11/2}$ GSA band at 979 nm. In the Fig. 3 is evident a red shift of the absorption edge of the $Ge_{25}Ga_{9.5}Sb_{0.5}S_{65}$ host matrix with increasing Yb^{3+} content.

The Judd-Ofelt phenomenological parameters for the Er^{3+} ions embedded in the $Ge_{25}Ga_{9.5}Sb_{0.5}S_{65}$ glassy host were found to be $\Omega_2=(12.58\pm1.10)\times10^{-20}$ cm^2, $\Omega_4=(3.25\pm1.28)\times10^{-20}$ cm^2 and $\Omega_6=(2.05\pm0.45)\times10^{-20}$ cm^2 which are comparable to similar chalcogenide glasses [21]. Root-mean-square (RMS) deviation between the theoretical and the experimental line strengths was 0.63×10^{-20} cm^2. The large value of the Ω_2 parameter can be related to a high degree of the covalent bonding around the Er^{3+} ions and in some extent to the asymmetry. The spectroscopic quality factor $\Omega_4/\Omega_6=1.59$ can be used as a prediction for the stimulated emission ability

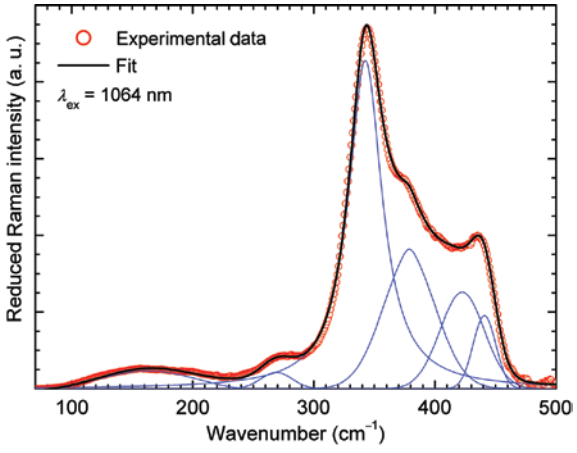

Fig. 2: Reduced Raman spectrum of the $(Ge_{0.25}Ga_{0.095}Sb_{0.005}S_{0.65})_{99.9}Er_{0.1}$ glass. (color online).

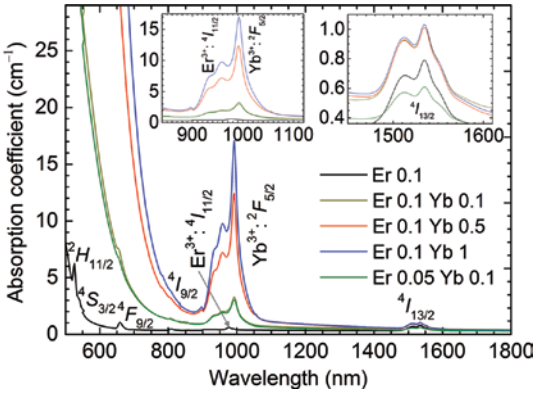

Fig. 3: The absorption coefficient of the $Ge_{25}Ga_{9.5}Sb_{0.5}S_{65}$: Er^{3+}/Yb^{3+} ChGs with labeled Er^{3+} and Yb^{3+} GSA transitions from respective levels $^4I_{15/2}$ and $^2F_{7/2}$ to the upper manifolds. (color online).

for such intra-4*f* transitions, where the first terms of doubly reduced matrix elements are negligible or zero. The calculated radiative transition probabilities, branching ratios and radiative lifetimes of selected Er^{3+} transitions are presented in Table 3.

The proposed UCPL mechanism in the Er^{3+}/Yb^{3+}-co-doped samples under 980 nm excitation wavelength is schematically drawn in the Fig. 4. The 980 nm wavelength excites the Er^{3+} and Yb^{3+} by the ground state absorption (GSA) into Er^{3+}: $^4I_{11/2}$ and Yb^{3+}: $^2F_{5/2}$ levels, respectively. Subsequently, the Er^{3+}: $^4F_{7/2}$ manifold can be populated: (1) by the excited state absorption (ESA) $^4I_{11/2} \rightarrow {}^4F_{7/2}$ within Er^{3+} ion, or (2) by the energy transfer

Table 3: Spontaneous electric dipole A_{ED} and magnetic dipole A_{MD} emission probabilities, branching ratios β and radiative lifetimes τ of the $(Ge_{0.25}Ga_{0.095}Sb_{0.005}S_{0.65})_{99.9}Er_{0.1}$ calculated by the Judd-Ofelt theory.

Transition	λ (nm)	A_{ED} (s^{-1})	A_{MD} (s^{-1})	β (%)	τ (ms)
$^2H_{11/2} \rightarrow {}^4I_{15/2}$	533	49255.0	0	96	0.020
$^4S_{3/2} \rightarrow {}^4I_{13/2}$	859	2055.7	0	26	0.404
$^4S_{3/2} \rightarrow {}^4I_{15/2}$	556	5500.3	0	69	0.125
$^4F_{9/2} \rightarrow {}^4I_{15/2}$	670	6926.6	0	91	0.131
$^4I_{9/2} \rightarrow {}^4I_{15/2}$	823	771.8	0	79	1.018
$^4I_{11/2} \rightarrow {}^4I_{15/2}$	1002	693.4	0	86	1.246
$^4I_{13/2} \rightarrow {}^4I_{15/2}$	1580	448.2	85.6	100	1.873

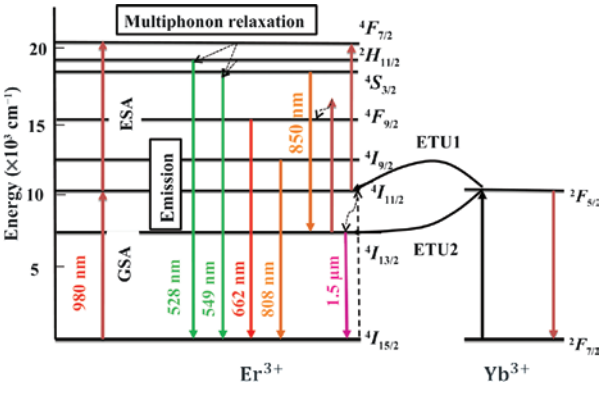

Fig. 4: Schematic energy level diagram for the Er^{3+}/Yb^{3+} -co-doped $Ge_{25}Ga_{9.5}Sb_{0.5}S_{65}$ glass with observed emissions and proposed mechanisms standing behind the UCPL emissions. (color online).

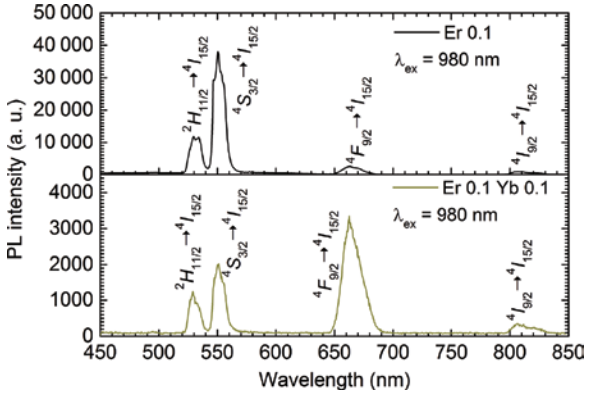

Fig. 5: UCPL emission spectra of the $(Ge_{0.25}Ga_{0.095}Sb_{0.005}S_{0.65})_{99.9}Er_{0.1}$ and the $(Ge_{0.25}Ga_{0.095}Sb_{0.005}S_{0.65})_{99.8}Er_{0.1}Yb_{0.1}$ glasses at pumping wavelength of 980 nm laser. (color online).

(ETU1) between Er^{3+} and Yb^{3+} ions as Er^{3+}: $^4I_{11/2}$, Yb^{3+}: $^2F_{5/2} \rightarrow Er^{3+}$: $^4F_{7/2}$, Yb^{3+}: $^2F_{7/2}$. The thermalized levels $^2H_{11/2}$ and $^4S_{3/2}$ responsible for the green UCPL will be populated from $^4F_{7/2}$ in particular by the multiphonon relaxation due to their small energy difference. On the other hand, the energy transfer (ETU2) Er^{3+}: $^4I_{13/2}$, Yb^{3+}: $^2F_{5/2} \rightarrow Er^{3+}$: $^4F_{9/2}$, Yb^{3+}: $^2F_{7/2}$ can be assumed as well promoting the Er^{3+} red UCPL $^4F_{9/2} \rightarrow {}^4I_{15/2}$. It should be noted that the ETU1 and ETU2 processes can originate between neighboring Er^{3+} ions (without Yb^{3+}) due to similar energy positions of the Er^{3+}: $^4I_{11/2}$ and Yb^{3+}: $^2F_{5/2}$. Revealing the UCPL dynamics is a difficult task and among the ChGs was recently studied in Ge-Ga-S: Er^{3+} ChGs [32, 33]. Moreover, experimentally observed Er^{3+}: $^4S_{3/2} \rightarrow {}^4I_{13/2}$ (≈850 nm) UCPL emission populating the $^4I_{13/2}$ level is promising for the Er^{3+}: $^4I_{13/2} \rightarrow {}^4I_{15/2}$ (≈1.5 μm) optical amplification.

The effect of Yb^{3+} addition to sensitize the UCPL emission was investigated for samples $(Ge_{0.25}Ga_{0.095}Sb_{0.005}S_{0.65})_{99.9-x}Er_{0.1}Yb_x$ ($x = 0$, 0.1, 0.5, 1) and $(Ge_{0.25}Ga_{0.095}Sb_{0.\ 005}S_{0.65})_{99.85}Er_{0.05}Yb_{0.1}$ at pumping wavelength of 980 nm. The UCPL emission spectra are presented in the Fig. 5 from the visible to the near-infrared spectral region. The addition of Yb^{3+} ions lowers the total UCPL emission intensity and promotes the red-to-green UCPL intensity ratio. This is probably because of a red shift of the absorption edge of glassy host matrix with Yb addition (Fig. 3) which promotes the absorption of the excitation light (due to the ESA, ETU processes) by host matrix. Thus, the co-doping of the $Ge_{25}Ga_{9.5}Sb_{0.5}S_{65}$: 0.1 at.% Er^{3+} ChGs by the Yb^{3+} ions is inefficient to improve the UCPL emission intensity.

Stokes and anti-Stokes (UCPL) PL spectra of the $(Ge_{0.25}Ga_{0.095}Sb_{0.005}S_{0.65})_{99.9}Er_{0.1}$ glass at pumping wavelengths of 490, 532, 810 and 980 nm are presented in Fig. 6. The observed emission bands at 529, 551, 660, 808, and 850 nm can be assigned to the Er^{3+}: $^2H_{11/2} \rightarrow {}^4I_{15/2}$, $^4S_{3/2} \rightarrow {}^4I_{15/2}$, $^4F_{9/2} \rightarrow {}^4I_{15/2}$, $^4I_{9/2} \rightarrow {}^4I_{15/2}$ and $^4S_{3/2} \rightarrow {}^4I_{13/2}$

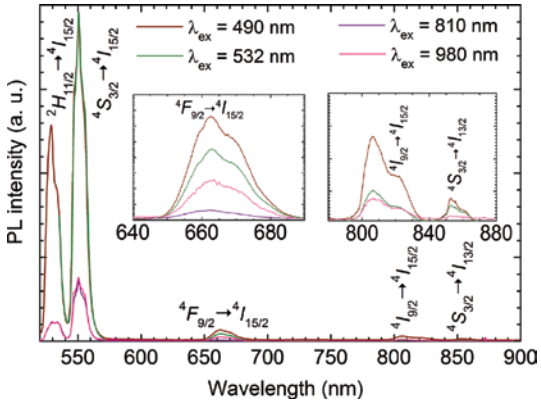

Fig. 6: Emission spectra of the $(Ge_{0.25}Ga_{0.095}Sb_{0.005}S_{0.65})_{99.9}Er_{0.1}$ glass measured at various excitation wavelengths λ_{ex}. (color online).

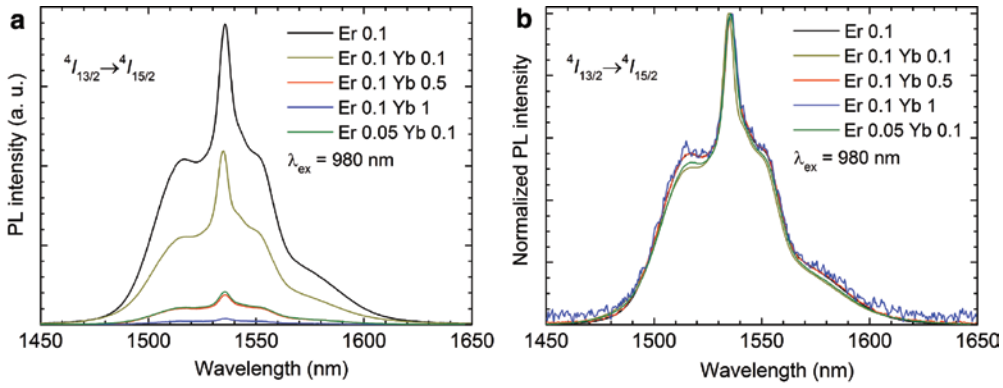

Fig. 7: (a) The PL Er^{3+}: $^4I_{13/2}\rightarrow{}^4I_{15/2}$ emission spectra and (b) the same normalized spectra of the $Ge_{25}Ga_{9.5}Sb_{0.5}S_{65}$: 0.1 or 0.05 at.% Er^{3+} ChGs co-doped with various concentrations of Yb^{3+} ions under 980 nm excitation. (color online).

electronic transitions, respectively. The PL emission intensities at 550 nm originating from $^4S_{3/2}\rightarrow{}^4I_{15/2}$ transitions are similar for excitation wavelength of 490 and 532 nm which directly excite the upper $^4F_{7/2}$ and $^2H_{11/2}$ levels. From these manifolds the $^4S_{3/2}$ level is populated by the multiphonon relaxation and thus, the emission characteristics are similar. On the other hand, the emissions at excitation wavelengths of 810 and 980 nm originate from the nonlinear UCPL processes and thus, they have lower intensity (approximately ≈5 times). However, the UCPL intensity is still sufficiently high, which makes these materials promising for the UCPL applications.

In addition, we investigated the ≈1.5 μm PL emission originating from Er^{3+}: $^4I_{13/2}\rightarrow{}^4I_{15/2}$ transitions at 980 nm pumping wavelength against Yb^{3+} content which is depicted in the Fig. 7. The PL emission intensity decreases with increasing Yb^{3+} content. This is probably due to the concentration quenching and/or due to UCPL processes depopulating the $^4I_{13/2}$ energy level. Thus, the present study demonstrates that the Yb^{3+} addition into $Ge_{25}Ga_{9.5}Sb_{0.5}S_{65}$: Er^{3+} ChGs does not lead to appreciable sensitization of the UCPL as well as 1.5 μm PL emissions. However, we believe that this drawback can be overcome by using the host material with larger optical band gap energy. Such promising materials can be chalcohalide or oxychalcogenide glasses where the trade-off between intra-4*f* electronic intensities, solubility of Er^{3+}/Yb^{3+} ions and optical band gap energy might be found.

Conclusions

Er^{3+}-doped and Er^{3+}/Yb^{3+}-co-doped $Ge_{25}Ga_{9.5}Sb_{0.5}S_{65}$ thermally stable chalcogenide glasses were synthesized by the melt-quenching technique. The Judd-Ofelt theory was used for calculation of the Er^{3+} intra-4*f* electronic transitions intensities. The $Ge_{25}Ga_{9.5}Sb_{0.5}S_{65}$ glass doped with 0.1 at.% Er^{3+} shows intense upconversion photoluminescence (UCPL) from green to near-infrared spectral region. The green UCPL emission is approximately 5 times lower than the green Stokes photoluminescence (PL) Stokes emission intensity, which makes this material attractive for the UCPL applications. However, it is presented that the Yb^{3+} ions sensitization is ineffective resulting in the decrease of the total UCPL emission intensity under 980 nm laser excitation. This is attributed to a red shift of the absorption edge of host matrix with Yb addition, which is merged with the upper Er^{3+} energy level manifolds $^4F_{7/2}$, $^2H_{11/2}$ and $^4S_{3/2}$. Moreover, the ≈1.5 μm PL emission intensity decreases with the increasing Yb content probably due to the concentration quenching. Thus, the addition of Yb^{3+} ions was shown to be inefficient to improve the UCPL and ≈1.5 μm PL, which could be overcome by the using of chalcohalide or oxychalcogenide glasses as host matrices. Thereafter, the observed Er^{3+}: $^4S_{3/2}\rightarrow{}^4I_{13/2}$ (≈850 nm) emission could be utilized for the optical amplification at ≈1.5 μm ($^4I_{13/2}\rightarrow{}^4I_{15/2}$) via upconversion processes.

Acknowledgments: Authors acknowledge the financial support from Grant Agency of Czech Science Foundation of the Czech Republic, project no. 15-07912S. This work was supported by the project CZ.1.05/4.1.00/11.0251 and by grant LM2015082 Center of Materials and Nanotechnologies from the Czech Ministry of Education, Youth and Sports of the Czech Republic.

References

[1] N. F. Mott, E. A. Davis. *Electronic Processes in Non-Crystalline Materials*, Clarendon, Oxford (1979).
[2] B. Bureau, X. H. Zhang, F. Smektala, J.-L. Adam, J. Troles, H. Ma, C. Boussard- Plèdel, J. Lukcas, P. Lucas, D. Le Coq, M. R. Riley, J. H. Simmons. *J. Non Cryst. Solid*. **276**, 345 (2004).
[3] T. Wagner, M. Frumar. "Optically-induced diffusion and dissolution of metals in amorphous chalcogenides", in *Photo-Induced Metastability in Amorphous Semiconductors*, A. V. Kolobov (Ed.), pp. 160–177, Wiley-VCH Verlag, Berlin (2003).
[4] V. G. Truong, B. S. Ham, A. M. Jurduc, B. Jacquier, J. Leperson, V. Nazabal, J. L. Adam. *Phys. Rev. B*. **74**, 184103 (2006).
[5] L. B. Shaw, B. Cole, P. A. Thielen, J. S. Sanghera, I. D. Aggarwal. *IEEE J Quantum Elec.* **48**, 1127 (2001).
[6] F. Prudenzano, L. Mescia, L. Allegretti, M. DeSario, F. Smektala, V. Mozain, V. Nazabal, J. Troles, J. L. Doualan, G. Canat, J. L. Adam, B. Boulard. *Opt. Mater.* **31**, 1292 (2009).
[7] A. V. Rode, A. Zakery, M. Samoc, R. B. Charters, E. G. Gamaly, B. Luther-Davies. *Appl. Surf. Sci.* **481**, 197 (2002).
[8] N. G. Boetti, J. Lousteau, D. Negro, E. Mura, G. Scarpignato, S. Abrate, D. Milanese. *Opt. Express*. **20**, 5409 (2012).
[9] F. Charpentier, B. Bureau, J. Troles, C. Boussard-Plédel, K. Michel-LePierres, F. Smektala, J.-L. Adam. *Opt. Mater.* **31**, 496 (2009).
[10] W. Length, R. M. McFarlane. *Opt. Photonics News*. **3**, 8 (1992).
[11] J. LePerson, F. Colas, C. Compere, M. Lehaitre, M.-L. Anne, C. Boussard-Plédel, B. Bureau, J.-L. Adam, S. Deputier, M. Guilloux-Viry. *Sens. Actuators*. **B130**, 771 (2008).
[12] F. Prudenzano, L. Mescia, L. Allegretti, V. Mozain, V. Nazabal, F. Smektala. *Opt. Mater.* **33**, 241 (2010).
[13] F. Prudenzano, L. Mescia, L. A. Allegretti, M. De Sario, T. Palmisano, F. Smektala, V. Mozain, V. Nazabal, J. Troles. *J. Non Cryst. Solids*. **355**, 1145 (2009).
[14] F. Rivera-Lopez, P. Babu, L. Jyothi, U. R. Rodriguez-Mendoza, I. R. Martin, C. K. Jayasankar, V. Lavin. *Opt. Mater.* **34**, 1235 (2012).
[15] J. D. B. Bradely, M. Pollanu. *Lasers Photon.* **5**, 368 (2011).
[16] M. Federighi, F. Di Pasquale. *IEEE Photonic Tech. L.* **7**, 303 (1995).
[17] E. Snitzer, R. Woodcock. *Appl. Phys. Lett.* **6**, 45 (1965).
[18] B. S. Reddy, H.-Y. Hwang, Y.-D. Jho, B. S. Ham, S. Sailaja, C. M. Reddy, B. V. Rao, S. J. Dhoble. *Ceram. Int.* **41**, 3684 (2015).
[19] J.-M. P. Delavaux, S. Granlund, O. Mizuhara, L. D. Tzeng, D. Barbier, M. Rattay, F. Saint André, A. Kevorkian. *IEEE Photonic Tech. L.* **9**, 247 (1997).
[20] Y. Guimond, J.-L. Adam, A.-M. Jurdyc, H. L. Ma, J. Mugnier, B. Jacquier. *J. Non Cryst. Solids*. **256, 257**, 378 (1999).
[21] L. Strizik, J. Zhang, T. Wagner, J. Oswald, T. Kohoutek, B. M. Walsh, J. Prikryl, R. Svoboda, C. Liu, B. Frumarova, M. Frumar, M. Pavlista, W. J. Park, J. Heo. *J. Lumin.* **147**, 209 (2014).
[22] J. Heo, J. M. Yoon, S. Y. Ryou. *J. Non Cryst. Solids*. **238**, 115 (1998).
[23] R. Shuker, R. W. Gammon. *Phys. Rev. Lett.* **25**, 222 (1970).
[24] W. Sellmeier. *Ann. Phys. Chem.* **143**, 271 (1871).
[25] B. M. Walsh. "Judd-Ofelt Theory: principles and practices", in *Advances in Spectroscopy for Lasers and Sensing*, B. Di Bartolo, O. Forte (Eds.), pp. 403–433, Springer, Netherlands (2006).
[26] P. Goldner, F. Auzel. *J. Appl. Phys.* **79**, 7972 (1996).
[27] B. R. Judd. *Phys. Rev.* **127**, 750 (1962).
[28] G. S. Ofelt. *J. Chem. Phys.* **37**, 511 (1962).
[29] W. T. Carnall, P. R. Fields, B. G. Wybourne. *J. Chem. Phys.* **42**, 3797 (1965).
[30] M. Wojdyr. *J. Appl. Crystallogr.* **43**, 1126 (2010).
[31] S. W. Yung, H. J. Lin, Y. Y Lin, R. K. Brow, Y. S. Lai, J. S. Horng, T. Zhang. *Mater. Chem. Phys.* **117**, 29 (2009).
[32] L. Strizik, V. Prokop, J. Hrabovsky, T. Wagner, T. Aoki. *J. Mater. Sci. Mater. El.* (2017). https://link.springer.com/article/10.1007/s10854-016-6306-3.
[33] T. Aoki, L. Strizik, J. Hrabovsky, T. Wagner. *J. Mater. Sci-Mater. El.* (2017). https://link.springer.com/article/10.1007/s10854-017-6363-2.